Research Square

Preprints are preliminary reports that have not undergone peer review.
They should not be considered conclusive, used to inform clinical practice,
or referenced by the media as validated information.

Kerr Photonics: Enhancing Quantum Teleportation

Sisay Belachew

sbelachew9@gmail.com

Oda Bultum University

Mohammed Kelif

Oda Bultum University

Firomsa Feyissa

Oda Bultum University

Research Article

Keywords: Kerr photonics, quantum teleportation, parametric coupling, EPR variance, teleportation fidelity, quantum communication

Posted Date: September 21st, 2026

DOI: https://doi.org/10.21203/rs.3.rs-10961021/v1

License: This work is licensed under a Creative Commons Attribution 4.0 International License.
Read Full License

Additional Declarations: No competing interests reported.

Version of Record: A version of this preprint was published at Optical and Quantum Electronics on October 21st, 2026. See the published version at https://doi.org/10.1007/s11082-026-09203-6.

Kerr Photonics: Enhancing Quantum Teleportation

Sisay Belachew[1*], Mohammed Kelif[2] and Firomsa Feyissa[3]

[1,2,3]Department of Physics, Oda Bultum University, Chiro, 226, Oromia, Ethiopia.

*Corresponding author(s). E-mail(s): sbelachew9@gmail.com;
Contributing authors: momahedkelifa@obu.edu.et;
firomsafeyissa@obu.edu.et;

Abstract

On this paper, we present a Kerr enhanced continuous variable quantum teleportation scheme based on a driven dissipative nondegenerate optical resonator that combines two mode parametric squeezing with intrinsic third-order Kerr nonlinearity. Right here by linearizing the quantum Langevin dynamics around the self consistent steady state intracavity fields and solving the associated continuous Lyapunov equation, we obtain the steady state covariance matrix and systematically characterize the resulting quantum correlations through logarithmic negativity, EPR variance, teleportation fidelity, and dynamical stability. With the assist of Kerr nonlinearity, parametric coupling, detuning, pump amplitude, and stability our results demonstrate that the quantum teleportation. our finding analysis the optimized stable regime supports teleportation fidelity above the classical benchmark, $\boldsymbol{F_{tel} > 0.5}$, establishing a direct connection between engineered Kerr mediated quantum correlations and operationally useful continuous variable state transfer. These results establish a promising compact platform for tunable entanglement generation and integrated quantum communication.

Keywords: Kerr photonics; quantum teleportation; parametric coupling; EPR variance; teleportation fidelity; quantum communication

1 Introduction

Quantum teleportation provides a mechanism for transferring an unknown quantum state from one physical system to another without physically transmitting the quantum state itself [1–4]. In optical platforms, continuous variable quantum teleportation is particularly attractive because quantum information can be encoded in the field

quadratures, enabling deterministic measurements and compatibility with established photonic communication technologies [5–9]. In realistic photonic systems, however, finite squeez ing, optical loss, detector inefficiency, environmental noise, and imperfect state preparation introduce additional noise and consequently limit the achievable fidelity [10, 11]. The development of compact and controllable photonic sources capable of generating strong nonclassical correlations is therefore a central requirement for scalable continuous variable quantum communication. The optical Kerr effect provides a natural mechanism for nonlinear photon photon interaction and and offers a route toward the generation and control of nonclassical optical states [12].

Optical Kerr nonlinearities provide an intensity dependent photon photon interaction and constitute one of the most important nonlinear mechanisms in integrated photonics [13, 14]. In resonant optical systems, the Kerr interaction can produce self phase modulation, nonlinear frequency shifts, four wave mixing, parametric amplification, and squeezing. In high quality factor resonators, the enhanced intracavity field can substantially strengthen these nonlinear effects, making Kerr photonics a promising platform for the generation and manipula tion of nonclassical states of light [15, 16]. These properties make Kerr nonlinear systems promising candidates for the development of integrated continuous variable quantum information technologies.

While continuous variable quantum teleportation offers a scalable framework for optical quantum communication using field quadratures, its practical performance remains fundamentally constrained by finite squeezing, optical dissipation, and environmental noise. To address this challenge, we introduce a theoretical model that combines a nondegenerate two mode parametric interaction with third order $\chi^{(3)}$ optical Kerr nonlinearities, establishing intrinsic nonlinear processes as a direct mechanism for state engineering.

With this idea, we consider a continuous variable quantum teleportation scheme as show in the schematic below figure 1, that integrates a driven dissipative two mode Kerr as the nonclassical resource generator powering the quantum channel between Alice and Bob. Within the resonator, an external coherent optical pump drives modes $\hat{a}$ and $\hat{b}$, engaging simultaneous Kerr induced self and cross phase modulations alongside two-mode parametric coupling to generate entangled squeezed states. Mode $\hat{a}$ propagates to Alice (the sender) to undergo a joint continuous variable Bell-state measurement with an unknown input state $|\psi_{\text{in}}\rangle$ using a 50:50 beam splitter and dual homodyne detectors. Simultaneously, mode $\hat{b}$ is transmitted to Bob (the receiver) [17]. Upon receiving Alice's classical measurement outcomes (x_m, p_m) over a classical communication link, Bob performs conditional quadrature displacement and electronic feed-forward processing on his mode to reconstruct the transferred state $|\psi_{\text{out}}\rangle$ with enhanced fidelity.

The primary novelty of this work lies in modeling these open system interaction dynamics by linearizing quantum fluctuations around steady state intracavity fields and solving the continuous Lyapunov equation. Through this approach, we systematically map the precise, dynamically stable operating regimes where cavity detunings, pump driving, and Kerr non linearities work synergistically to maximize bipartite continuous variable entanglement (logarithmic negativity), suppress EPR quadrature noise, and optimize operational teleportation fidelity.

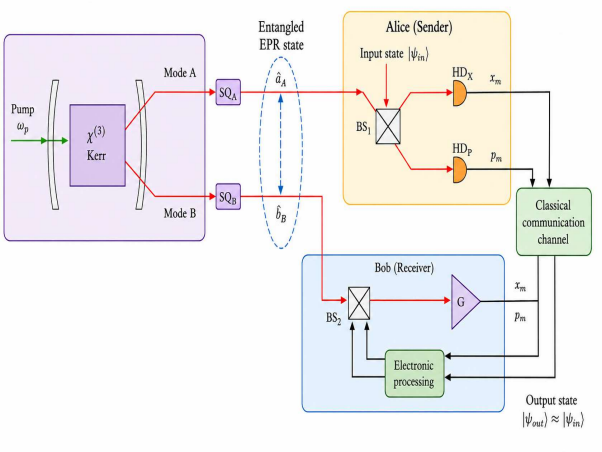


Fig. 1 Schematic represents a Kerr photonics enhanced continuous variable quantum teleportation. A coherent pump drive activates a $\chi^{(3)}$ nonlinear optical cavity, which simultaneously engages Kerr self and cross phase modulation and nondegenerate two mode parametric interaction to generate an entangled squeezed vacuum state of modes $\hat{a}$ and $\hat{b}$. Mode $\hat{a}$ propagates to the Sender (Alice), where it undergoes joint measurement with an unknown input state $|\psi_{\rm in}\rangle$. Mode $\hat{b}$ propagates to the Receiver (Bob), who uses classical feed forward data (x_m, p_m) and quadrature displacement to reconstruct the transferred state $|\psi_{\rm out}\rangle$ with high fidelity

2 Hamiltonian and Master Equation

For the quantum dynamics of the source the total Hamiltonian combines detunings $(\Delta_{a,b})$, Kerr coefficients $(K_{a,b})$, coherent pump $(\mathcal{E})$, and parametric coupling (Λ):

$$\hat{H} = \underbrace{\hbar\Delta_a \hat{a}^\dagger \hat{a} + \hbar\Delta_b \hat{b}^\dagger \hat{b}}_{\hat{H}_{\rm free}} + \underbrace{\frac{\hbar K_a}{2} a^{\dagger 2} a^2 + \frac{\hbar K_b}{2} b^{\dagger 2} b^2}_{\hat{H}_{\rm kerr}} + \underbrace{i\hbar\mathcal{E}(a^\dagger - a)}_{\hat{H}_{\rm drive}} + \underbrace{i\hbar\Lambda\left(a^\dagger b^\dagger - ab\right)}_{\hat{H}_{\rm TMS}} \quad (1)$$

Because the optical resonator is an open quantum system, photon losses must be included. The density matrix obeys the Lindblad master [18] equation:

$$\dot{\rho} = -\frac{i}{\hbar}[H, \rho] + \kappa_a \mathcal{D}[a]\rho + \kappa_b \mathcal{D}[b]\rho, \quad (2)$$

where κ_a and κ_b are the decay rates of the two optical modes. where the dissipator for mode $\hat{a}$ is

$$\mathcal{D}[a]\rho = a\rho a^\dagger - \frac{1}{2}a^\dagger a\rho - \frac{1}{2}\rho a^\dagger a. \quad (3)$$

For a symmetric system, we consider the decay rates of the two optical mode as $\kappa_a = \kappa_b = \kappa$. The corresponding Heisenberg Langevin equations are

$$\dot{a} = -\left(\frac{\kappa_a}{2} + i\Delta_a\right) a - iK_a a^\dagger a a + \mathcal{E} + \Lambda b^\dagger + \sqrt{\kappa_a}\, a_{\rm in} \quad (4)$$

$$\dot{b} = -\left(\frac{\kappa_b}{2} + i\Delta_b\right) b - iK_b b^\dagger bb + \Lambda a^\dagger + \sqrt{\kappa_b}\, b_{\text{in}}. \tag{5}$$

Here a_{in} and b_{in} are the input noise operators. For vacuum input fields, $\left\langle a_{\text{in}}(t) a_{\text{in}}^\dagger(t') \right\rangle = \delta(t-t')$ and $\left\langle b_{\text{in}}(t) b_{\text{in}}^\dagger(t') \right\rangle = \delta(t-t')$

3 Linearized Dynamics and Quantum Correlations

To analyze quantum fluctuations around the operating point, the optical operators are decomposed into their steady state coherent amplitudes ($\hat{a} = \alpha_s + \delta\hat{a}$, $\hat{b} = \beta_s + \delta\hat{b}$).

The steady state amplitudes satisfy

$$0 = -\left(\frac{\kappa_a}{2} + i\Delta_a\right) \alpha_s - iK_a|\alpha_s|^2\alpha_s + \mathcal{E} + \Lambda\beta_s^* \tag{6}$$

$$0 = -\left(\frac{\kappa_b}{2} + i\Delta_b\right) \beta_s - iK_b|\beta_s|^2\beta_s + \Lambda\alpha_s^*. \tag{7}$$

The Kerr interaction produces an intensity-dependent frequency shift [19]. Therefore, the effective detunings are $\zeta_a = \Delta_a + 2K_a|\alpha_s|^2$and $\zeta_b = \Delta_b + 2K_b|\beta_s|^2$. The Kerr induced parametric coefficients are $\eta_a = K_a\alpha_s^2$,and $\eta_b = K_b\beta_s^2$. The Linearized Hamiltonian of our system that used determine second order in the quantum fluctuations is

$$\begin{aligned} H_{\text{lin}} = {} & \hbar\zeta_a \delta a^\dagger \delta a + \hbar\zeta_b \delta b^\dagger \delta b + \frac{\hbar}{2}\left(\eta_a \delta a^{\dagger 2} + \eta_a^* \delta a^2\right) \\ & + \frac{\hbar}{2}\left(\eta_b \delta b^{\dagger 2} + \eta_b^* \delta b^2\right) + i\hbar\Lambda\left(\delta a^\dagger \delta b^\dagger - \delta a \delta b\right). \end{aligned} \tag{8}$$

The corresponding linearized Langevin equations are

$$\delta\dot{a} = -\left(\frac{\kappa_a}{2} + i\zeta_a\right) \delta a - i\eta_a \delta a^\dagger + \Lambda\delta b^\dagger + \sqrt{\kappa_a}\, a_{\text{in}} \tag{9}$$

$$\delta\dot{b} = -\left(\frac{\kappa_b}{2} + i\zeta_b\right) \delta b - i\eta_b \delta b^\dagger + \Lambda\delta a^\dagger + \sqrt{\kappa_b}\, b_{\text{in}}. \tag{10}$$

The amplitude and phase quadratures are defined by

$$\delta X_a = \frac{\delta a + \delta a^\dagger}{\sqrt{2}}, \qquad \delta P_a = \frac{\delta a - \delta a^\dagger}{i\sqrt{2}}, \tag{11}$$

$$\delta X_b = \frac{\delta b + \delta b^\dagger}{\sqrt{2}}, \qquad \delta P_b = \frac{\delta b - \delta b^\dagger}{i\sqrt{2}}. \tag{12}$$

with the fluctuation vector $\mathbf{u} = (\delta X_a, \delta P_a, \delta X_b, \delta P_b)^T$ and the linearized Langevin equations can then be expressed as $\dot{\mathbf{u}} = A\mathbf{u} + \mathbf{n}$. where, the noise vector is

$$\mathbf{n} = \begin{pmatrix} \sqrt{\kappa_a} X_a^{\text{in}} \\ \sqrt{\kappa_a} P_a^{\text{in}} \\ \sqrt{\kappa_b} X_b^{\text{in}} \\ \sqrt{\kappa_b} P_b^{\text{in}} \end{pmatrix}. \tag{13}$$

The complete matrix A simplifies to

$$A = \begin{pmatrix} -\kappa_a/2 & \zeta_a & \Lambda_x & 0 \\ -\zeta_a & -\kappa_a/2 & 0 & -\Lambda \\ \Lambda_x & 0 & -\kappa_b/2 & \zeta_b \\ 0 & -\Lambda_p & -\zeta_b & -\kappa_b/2 \end{pmatrix}. \tag{14}$$

For an ideal symmetric two mode squeezing interactio, $\Lambda_x = \Lambda_p = \Lambda$. For vacuum input noise, $\left\langle X_j^{\text{in}}(t) X_j^{\text{in}}(t') \right\rangle = \frac{1}{2}\delta(t-t')$, and $\left\langle P_j^{\text{in}}(t) P_j^{\text{in}}(t') \right\rangle = \frac{1}{2}\delta(t-t')$.

Therefore, diffusion matrix is

$$D = \frac{1}{2} \begin{pmatrix} \kappa_a & 0 & 0 & 0 \\ 0 & \kappa_a & 0 & 0 \\ 0 & 0 & \kappa_b & 0 \\ 0 & 0 & 0 & \kappa_b \end{pmatrix}. \tag{15}$$

The system is dynamically stable when all eigenvalues of the drift matrix have negative real parts [20]:

$$\Gamma_{\text{stab}} = -\max_j \text{Re}[\lambda_j(A)] \tag{16}$$

This condition is particularly important because increasing the Kerr nonlinearity or the parametric gain does not indefinitely improve the entanglement. Beyond a certain regime, the system can become dynamically unstable. The steady state quantum fluctuations are characterized by the covariance matrix

$$V_{ij} = \frac{1}{2} \left\langle u_i u_j + u_j u_i \right\rangle. \tag{17}$$

The covariance matrix is written in block form as

$$V = \begin{pmatrix} V_a & C \\ C^T & V_b \end{pmatrix}. \tag{18}$$

For a stable system, the steady-state covariance matrix is obtained from the Lyapunov equation

$$AV + VA^T = -D. \tag{19}$$

4 Entanglement and Quantum Teleportation matrics

Continuous variable (CV) quantum teleportation provides a direct operational test of the quantum correlations generated by the two-mode entangled resource. The connection to teleportation is particularly direct. For unity gain continuous-variable teleportation, the amplitude and phase teleportation errors are given by the EPR combinations [21].

$$X_{\text{out}} - X_{\text{in}} = X_b - X_a, \qquad P_{\text{out}} - P_{\text{in}} = P_b + P_a. \tag{20}$$

a. Einstein Podolsky Rosen (EPR) Variance

Measures joint quadrature correlations determining the continuous variable teleportation noise floor [22]:

$$V_{\mathrm{EPR}} = \frac{1}{2}\left[\langle X_-^2\rangle + \langle P_+^2\rangle\right]. \tag{21}$$

Suppression of EPR variance below the shot-noise limit ($V_{\mathrm{EPR}} < 1$) reflects strong non-classical Einstein-Podolsky-Rosen correlations. For the commonly adopted EPR combinations [23], $N_X = \langle (X_b - X_a)^2 \rangle$, and $N_P = \langle (P_b + P_a)^2 \rangle$. In terms of the covariance matrix elements, $N_X = V_{X_a X_a} + V_{X_b X_b} 2V_{X_a X_b}$ and $N_P = V_{P_a P_a} + V_{P_b P_b} + 2V_{P_a P_b}$. For a symmetric teleportation channel, $N_X = N_P = N$. The quantity N therefore provides a direct operational measure of the residual noise imposed by the imperfect entangled resource. In the present quadrature convention, if

$$V_{\mathrm{EPR}} = \frac{1}{2}\langle (X_b - X_a)^2 \rangle = \frac{1}{2}\langle (P_b + P_a)^2 \rangle, \tag{22}$$

As a result, $N = 2V_{\mathrm{EPR}}$, the EPR variance provides a direct bridge between the microscopic quantum correlations of the resource and the macroscopic performance of the teleportation channel.

b. Teleportation Fidelity

For a coherent state input and a unity gain symmetric Gaussian teleportation channel transferring unknown coherent input states, the maximum teleportation fidelity [24] is evaluated as

$$F_{\mathrm{tel}} = \frac{1}{\sqrt{(1+N_X)(1+N_P)}} \tag{23}$$

For a symmetric channel,

$$F_{\mathrm{tel}} = \frac{1}{1+N}. \tag{24}$$

Using $N = 2V_{\mathrm{EPR}}$, one obtains

$$F_{\mathrm{tel}} = \frac{1}{1+2V_{\mathrm{EPR}}}. \tag{25}$$

A teleportation fidelity exceeding the no-cloning classical benchmark ($F_{\mathrm{tel}} > 0.5$) verifies non-classical continuous-variable state transfer.

c. Logarithmic Negativity

Quantifies bipartite entanglement via the symplectic spectrum of the partially transposed covariance matrix used from equatio 18; where $\widetilde{\nu}_- = \sqrt{\frac{\Sigma - \sqrt{\Sigma^2 - 4\det V}}{2}}$ is the smallest symplectic eigenvalue of the partially transposed covariance matrix with invariant matrix $\Sigma = \det A + \det B - 2\det C$ for a block partitioned covariance matrix V. We employ the logarithmic negativity to quantify the entanglement can be defined as [25]

$$E_N = \max\left[0, -\log_2\left(2\widetilde{\nu}_-\right)\right]. \tag{26}$$

According to the definition of equation 26, certifies bipartite entanglement if $E_N > 0$.

5 Numerical results and Discussions

To evaluate the operational advantage of the proposed Kerr-photonic architecture for continuous variable quantum teleportation, we numerically solve the continuous Lyapunov equation to obtain the steady-state covariance matrix V across diverse parameter spaces. By using steady-state covariance matrix, we can analysis the logarithmic negativity E_N (quantifying bipartite entanglement), the EPR quadrature variance V_{EPR} (quantifying joint quadrature noise), and the coherent state teleportation fidelity

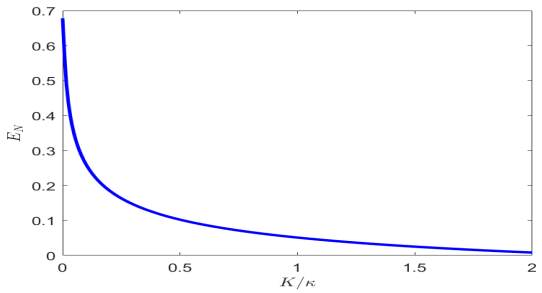


Fig. 2 Logarithmic negativity versus Kerr nonlinearity for fixed parametric coupling ($\Lambda/\kappa = 0.30$), zero detuning ($\Delta/\kappa = 0$), normalized driving amplitude ($\varepsilon/\kappa = 2.0$), and cavity decay rate (κ)

Figure 2 shows how the intrinsic Kerr nonlinearity shapes the bipartite optical resource state by self consistently modifying both the steady state intracavity fields and the Gaussian fluctuation matrix. The variation of E_N with K/κ shows how the Kerr interaction modifies the quantum correlations generated by the coupled system. Figures 2 and 3 illustrates how increasing the Kerr nonlinearity influences on quantum information quantities logarithmic negativity E_N and EPR variance V_{EPR} on the normalized Kerr coefficient K/κ. With this idea, as K/κ increases from zero, E_N exhibits a sharp initial drop, while V_{EPR} rapidly rises above the shot-noise limit ($V_{\mathrm{EPR}} > 1$). Correspondingly, Figure 4 show that the coherent state teleportation fidelity F_{tel} falls below the classical benchmark threshold ($F_{\mathrm{tel}} \leq 0.5$) for higher Kerr strengths. This indicates that uncompensated Kerr nonlinearity disrupts the resonance condition and drives the system toward dynamical instability, highlighting that the physically meaningful operational window is restricted to the stable regime where $E_N > 0$ and $V_{\mathrm{EPR}} < 1$.

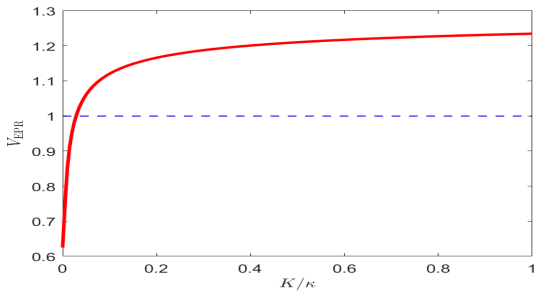


Fig. 3 EPR variance versus Kerr nonlinearity fixed parameters ($\Lambda/\kappa = 0.30$), ($\Delta/\kappa = 0$), and ($\varepsilon/\kappa = 2.0$)

As seen figure 3, the EPR variance provides a more directly operational measure of the joint quadrature correlations relevant to continuous variable quantum communication. The smaller V_EPR means stronger EPR type correlations. Thus, regions below at $V_{\mathrm{EPR}} = 1$ line correspond to enhanced EPR correlations. The Kerr interaction changes these correlations indirectly through the nonlinear steady state and the Kerr induced. If the curve decreases as K increases, the result means that the Kerr interaction is producing a state with increasingly suppressed joint-quadrature fluctuations.

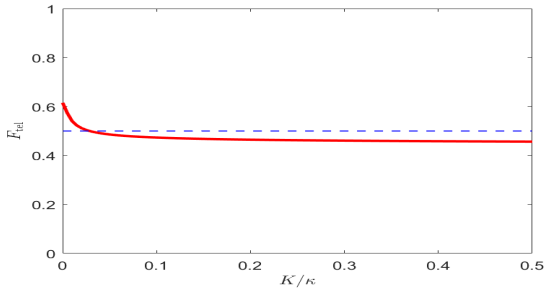


Fig. 4 Teleportation fidelity versus Kerr nonlinearity for fixed parametric coupling ($\Lambda/\kappa = 0.30$), zero detuning ($\Delta/\kappa = 0$), and driving amplitude ($\varepsilon/\kappa = 2.0$).

Figure 4 demonstrates that the coherent state teleportation fidelity F_{tel} falls below the classical benchmark threshold ($F_{\mathrm{tel}} \leq 0.5$) for higher Kerr strengths. This indicates that uncompensated Kerr nonlinearity disrupts the resonance condition and drives the system toward dynamical instability, highlighting that the physically meaningful operational window is restricted to the stable regime where $E_N > 0$ and $V_{\mathrm{EPR}} < 1.0$. The dashed line at $F_{\mathrm{tel}} = 0.5$ denotes the classical coherent-state benchmark. Therefore, $F_{\mathrm{tel}} > 0.5$ indicates performance beyond the classical limit.

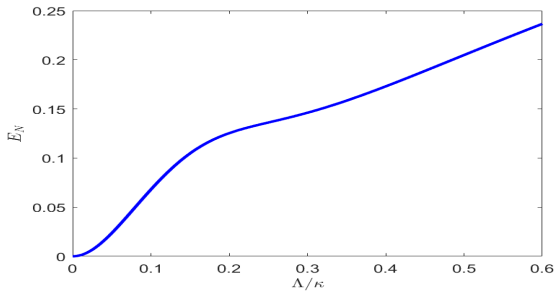


Fig. 5 Logarithmic negativity versus parametric coupling , with the Kerr nonlinear strength fixed at ($K/\kappa = 0.30$), zero detuning ($\Delta/\kappa = 0$), and driving amplitude ($\varepsilon/\kappa = 2.0$).

Figure 5, result shows the dependence of bipartite optical entanglement on the strength of the two-mode parametric interaction. Thus, increasing Λ generally strengthens the mechanism responsible for two-mode squeezing and entanglement. As seen from Figure 5, increasing Λ/κ yields a monotonic increase in logarithmic negativity E_N, demonstrating that stronger parametric interactions directly reinforce non-classical correlations between modes $\hat{a}$ and $\hat{b}$.

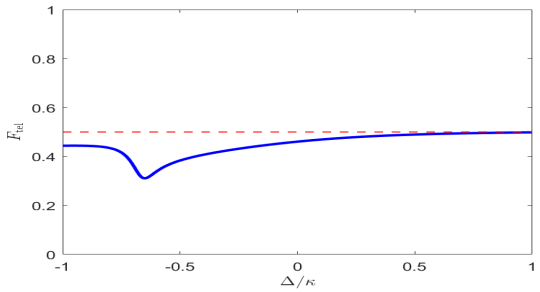


Fig. 6 Teleportation fidelity versus detuning for fixed Kerr nonlinear strength ($K/\kappa = 0.30$), parametric coupling ($\Lambda/\kappa = 0.30$), and driving amplitude ($\varepsilon/\kappa = 2.0$)

However, the efficacy of this interaction is strongly governed by the optical cavity detuning Δ/κ. Figure 6 reveals the teleportation fidelity F_{tel} as a function of detuning. Therefore, the Kerr interaction effectively shifts the resonance condition. This means that the optimal teleportation performance does not necessarily occur at $\Delta = 0$. Instead, the maximum can occur at a Kerr shifted resonance condition where the effective detuning and nonlinear squeezing terms cooperate most efficiently with the parametric coupling. At this optimal point, the Kerr-induced frequency shift ($2K|\alpha_s|^2$) perfectly counterbalances the bare cavity detuning, allowing the parametric driving and nonlinear squeezing terms to cooperate constructively and minimize EPR quadrature noise.

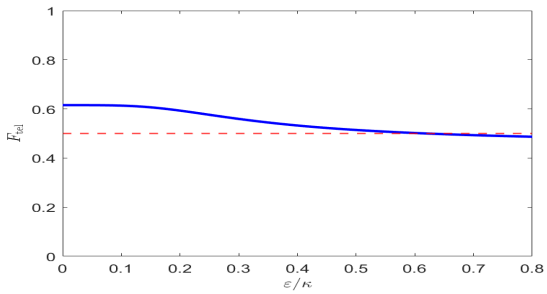


Fig. 7 Teleportation fidelity versus pump amplitude for fixed Kerr nonlinear strength ($K/\kappa = 0.30$), parametric coupling ($\Lambda/\kappa = 0.30$), and zero detuning ($\Delta/\kappa = 0$).

The amplitude of the coherent driving laser $\mathcal{E}/\kappa$ controls the intracavity photon intensity and dictates the strength of the nonlinear fluctuations. As shown in Figure 7, F_{tel} displays a clear non-monotonic trend with respect to $\mathcal{E}/\kappa$. At weak pumping ($\mathcal{E}/\kappa < 0.2$), the intracavity field is insufficient to activate meaningful Kerr-assisted squeezing, yielding a low teleportation fidelity. As pump power increases, F_{tel} peaks above the classical limit ($F_{\text{tel}} > 0.5$) before gradually declining due to excessive nonlinear phase shifts. This confirms the existence of an optimal pump operating point for CV teleportation. Thus, the maximum of Figure 7 identifies a possible optimal pump operating point, rather than simply implying that larger pump power is always better.

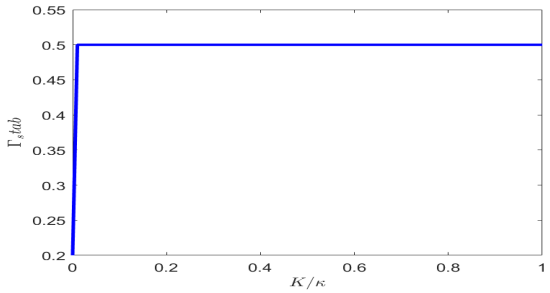


Fig. 8 Stability margin versus Kerr nonlinearity, for fixed parametric coupling ($\Lambda/\kappa = 0.30$), zero detuning ($\Delta/\kappa = 0$), and driving amplitude ($\varepsilon/\kappa = 2.0$), where (λ_j) are the eigenvalues of the linearized drift matrix.

Figure 8 show the dynamical stability margin across the parameter space. The system maintains a constant, positive stability margin ($\Gamma_{\text{stab}} = 0.5\kappa$), verifying that all linearized fluctuations remain dynamically stable. A positive Γ_{stab} means that all eigenvalues have negative real parts and the steady state is dynamically stable. By operating within this stable non linear regime, Kerr microresonators effectively suppress teleportation noise and deliver enhanced continuous-variable state transfer.

6 conclusion

In this work, we studya Kerr enhanced continuous variable quantum teleportation scheme based on a driven dissipative nondegenerate optical resonator that combines two mode parametric squeezing with intrinsic third-order Kerr nonlinearit. By combining a nondegenerate two mode parametric interaction with intrinsic Kerr nonlinearities for generating and engineering bipartite nonclassical correlations directly within a compact optical resonator. Starting from the full nonlinear Hamiltonian and the corresponding Lindblad master equation, we linearized the quantum dynamics around the steady-state intracavity fields and characterized the resulting Gaussian fluctuations through the covariance matrix formalism and the Lyapunov equation. Our results show that Kerr nonlinearity, parametric coupling, detuning, and optical driving constitute jointly tunable control parameters for engineering an optimized continuous variable quantum teleportation channel. These findings position driven Kerr mediated as promising crucial for compact and potentially scalable integrated quantum photonic schemes, particularly where efficient generation, manipulation, and transfer of continuous variable quantum states are required for quantum communication networks.

Author contributions

Sisay Belachew, as the corresponding author, Conceptualization, Data curation, Formal Analysis, Software, Investigation, Methodology, Writing- original draft, Writing-review and editing, critically revised the manuscript for important intellectual content, and reviewed and edited the final manuscript. Firomsa Feyissa and Mohammed Kelif conducted manuscript editing , Visualization and validated the data analysis. All authors read and approved the final manuscript.

Declarations

Ethical Statement This study is entirely theoretical and computational and does not involve human participants, human subjects, animals, or human-derived materials. Therefore, ethical approval was not required.
Consent to Participate and Consent to Publish Not applicable. This study does not involve human participants or individual level personal data. Therefore, consent to participate and consent to publish are not applicable. **Funding** The authors declare that no funds, grants, or other financial support were received during the preparation of this manuscript.
Conflict of interest The authors declare no competing interests.
Data Availability The datasets generated and analyzed during the current study are available from the corresponding author upon reasonable request.

References

[1] Hu, X. M., Guo, Y., Liu, B. H., Li, C. F., & Guo, G. C. (2023). Progress in quantum teleportation. Nature Reviews Physics, 5(6), 339-353.

[2] Cacciapuoti, A. S., Caleffi, M., Van Meter, R., & Hanzo, L. (2020). When entanglement meets classical communications: Quantum teleportation for the quantum internet. IEEE Transactions on Communications, 68(6), 3808-3833.

[3] Qiu, J., Liu, Y., Hu, L., Wu, Y., Niu, J., Zhang, L., ... & Yu, D. (2025). Deterministic quantum state and gate teleportation between distant superconducting chips. Science Bulletin, 70(3), 351-358.

[4] Ma, Y. B., Fan, Y. R., Song, R. Y., Zhao, Y. Z., Liu, Y. Y., Shen, S., ... & Zhou, Q. (2026). Quantum Teleportation toward the Quantum Internet: A Concise Review. arXiv preprint arXiv:2607.25395.

[5] Gewers, F. L. (2025). Unconditional quantum teleportation of multi-color continuous-variable states: from near-infrared to telecommunications bands (Doctoral dissertation, Universidade de São Paulo).

[6] Pirandola, S., Eisert, J., Weedbrook, C., Furusawa, A., & Braunstein, S. L. (2015). Advances in quantum teleportation. Nature Photonics, 9(10), 641-652.

[7] Wang, H., Ralph, T. C., Renema, J. J., Lu, C. Y., & Pan, J. W. (2025). Scalable photonic quantum technologies. Nature Materials, 24(12), 1883-1897.

[8] Koudia, S., Oleynik, L., Bayraktar, M., Rehman, J. U., & Chatzinotas, S. (2025). Physical-layer aspects of quantum communications: A survey. IEEE Communications Surveys & Tutorials, 28, 4429-4457.

[9] Motaharifar, M., Hasani, M., & Kaatuzian, H. (2025). A survey on continuous variable quantum key distribution for secure data transmission: Toward the future of secured quantum-networks. Quantum Information & Computation, 25(2), 175-194.

[10] Labbé, F., Ekici, Ç., Zhdanov, I., Muthali, A. L., Oxenløwe, L. K., & Ding, Y. (2025). Thin-film lithium niobate quantum photonics: review and perspectives. Advanced Photonics, 7(4), 044002-044002.

[11] Zhu, H., Chen, T., Ma, H., Zhao, Z., Guo, J., Liang, Q., ... & Yang, J. (2026). Recent progress towards large-scale integrated photonic quantum computation. npj Nanophotonics, 3(1), 20.

[12] Dutt, A., Mohanty, A., Gaeta, A. L., & Lipson, M. (2024). Nonlinear and quantum photonics using integrated optical materials. Nature Reviews Materials, 9(5), 321-346.

[13] Geng, W., Fang, Y., Wang, Y., Bao, C., Liu, W., Pan, Z., & Yue, Y. (2024). Nonlinear photonics on integrated platforms. Nanophotonics, 13(18), 3253-3278.

[14] Dutt, A., Mohanty, A., Gaeta, A. L., & Lipson, M. (2024). Nonlinear and quantum photonics using integrated optical materials. Nature Reviews Materials, 9(5), 321-346.

[15] Liu, H. (2026). Physics and Engineering of Kerr-Nonlinear Microresonators for Integrated Light Sources (Doctoral dissertation, University of Colorado at Boulder).

[16] Pontula, S. (2024). Broadband single and multimode quantum light generation using optical nonlinearities (Doctoral dissertation, Massachusetts Institute of Technology).

[17] Bianchi, L., Marconi, C., & Bacco, D. (2026). Bell state measurements in quantum optics: A review of recent progress and open challenges. Quantum Science and Technology, 11(2), 023001.

[18] Fazio, R., Keeling, J., Mazza, L., & Schirò, M. (2025). Many-body open quantum systems. SciPost Physics Lecture Notes, 099.

[19] Chanana, G. (2025). Exploring Kerr Medium and Stark Shift Effects on Two-Atom, Two-Mode Field Interactions for Quantum State Control. International Journal of Theoretical Physics, 64(10), 280.

[20] Leipholz, H. (2013). Stability theory: An introduction to the stability of dynamic systems and rigid bodies. Springer-Verlag.

[21] Shi, S., Wang, Y., Tian, L., Li, W., Wu, Y., Wang, Q., ... & Peng, K. (2023). Continuous variable quantum teleportation network. Laser & Photonics Reviews, 17(2), 2200508.

[22] Abdo, B., Shanks, W., Jinka, O., Rozen, J. R., & Orcutt, J. (2025). Teleportation and entanglement swapping of continuous quantum variables of microwave radiation. Physical Review X, 15(3), 031075.

[23] Zhao, J., Jeng, H., Conlon, L. O., Tserkis, S., Shajilal, B., Liu, K., ... & Lam, P. K. (2023). Enhancing quantum teleportation efficacy with noiseless linear amplification. Nature Communications, 14(1), 4745.

[24] Cho, K., Kim, B., & Bang, J. (2026). Universality cost of non-Gaussian enhancement in continuous-variable quantum teleportation: A fidelity–deviation trade-off. arXiv preprint arXiv:2604.20103.

[25] Belachew, S., & Feyissa, F. (2025). Enhancing bipartite entanglement via optical parametric amplifier in an optomechanical device. Optics, 13(1), 1-8.